https://ntrs.nasa.gov/search.jsp?R=19930086241 2020-06-17T13:18:35+00:00Z

CASE FILE
COPY

NACA RM E50F12

NACA

RESEARCH MEMORANDUM

INVESTIGATION OF PERFORATED CONVERGENT-DIVERGENT DIFFUSERS WITH INITIAL BOUNDARY LAYER

By Maynard I. Weinstein

Lewis Flight Propulsion Laboratory
Cleveland, Ohio

NATIONAL ADVISORY COMMITTEE
FOR AERONAUTICS
WASHINGTON

August 15, 1950

NATIONAL ADVISORY COMMITTEE FOR AERONAUTICS

RESEARCH MEMORANDUM

INVESTIGATION OF PERFORATED CONVERGENT-DIVERGENT DIFFUSERS WITH INITIAL BOUNDARY LAYER

By Maynard I. Weinstein

SUMMARY

An investigation of mass-flow and total-pressure recovery characteristics of perforated convergent-divergent supersonic diffusers operating with initial boundary layer has been conducted at a Mach number of 1.90 at the NACA Lewis laboratory. Boundary layer was established by use of cylindrical inlets, approximately 2, 3, and 4 inlet diameters in length, affixed to diffusers that ranged in contraction ratio from 1.40 to 1.59. Peak total-pressure recovery and supercritical recovered mass flow were decreased a maximum of approximately 2 percent by the use of the longest inlets.

Combinations of cylindrical inlets, perforated supersonic diffusers, and a subsonic diffuser were evaluated as simulated wind tunnels having second throats. Comparisons made with noncontracted configurations of similar scale indicated operating power reductions of at least 25 percent based on a conservative approximation to the power required for bleeding mass flow through the diffuser perforations. These reductions were accomplished at operating total-pressure ratios of less than 1.2 and with removal through the perforations of less than 8 percent of the mass flow of the simulated test sections.

INTRODUCTION

Perforated convergent-divergent supersonic diffusers with their high total-pressure recoveries have possible application as aircraft engine diffusers and wind-tunnel second throats. In the tunnel application, they allow contracted fixed-wall configurations that avoid starting limitations and combine low operating pressure ratios with excellent flow stability. Characteristics of perforated diffusers for conditions of negligible boundary layer at the diffuser inlets are reported in references 1 and 2. For wind-tunnel applications the diffusers will encounter appreciable entrant boundary layer. A limited investigation has therefore

been conducted at the NACA Lewis laboratory to determine the effect of the presence of initial boundary layer on the mass-flow and total-pressure characteristics of this type of diffuser and to evaluate the over-all efficiency of the perforated diffuser as a second throat in a supersonic wind tunnel.

The investigation was conducted using diffusers submerged in the free air stream of the 18- by 18-inch supersonic tunnel at a free-stream Mach number of 1.90. The boundary layer at the diffuser inlets was induced and controlled by lengths of cylindrical tubes attached to the inlets. A series of diffuser contraction ratios and perforation distributions were included in the investigation.

The characteristics of cylindrical inlets attached directly to the subsonic diffuser were also investigated. These data were used in evaluating the merits of the perforated convergent-divergent diffusers for applications as wind-tunnel second throats as referred to similar scale, noncontracted configurations.

SYMBOLS

The following symbols are used in this report:

A	total perforated area of diffuser summed from throat
C	cylindrical length upstream of diffuser convergence, inches
c_p	specific heat at constant pressure
D	inlet diameter of test configuration, inches
K	power factor, ratio of total operating power requirement of simulated wind-tunnel configuration to theoretical power requirement of normal shock at inlet Mach number and mass flow
L	total length of test configuration upstream of subsonic diffuser, inches
l	length of perforated diffuser including throat, inches
M	Mach number
m	mass rate of air flow
P	total pressure

p static pressure

S cross-sectional area of diffuser

T stagnation temperature

x position of shock in cylinder measured from entrance of subsonic diffuser, inches

y position of shock in cylinder measured from cylinder inlet, inches

γ ratio of specific heat at constant pressure to specific heat at constant volume

η ratio of power requirement of simulated wind tunnel with second throat to that of similar noncontracted configuration (ratio of respective power factors K)

Subscripts:

b bleed

1 inlet of test configuration

2 throat of perforated diffuser

3 discharge duct

APPARATUS AND PROCEDURE

The investigation was conducted at the NACA Lewis laboratory in the 18- by 18-inch supersonic tunnel at a Mach number of 1.90 and a Reynolds number of 3.3×10^6 per foot. Principal dimensions of the complete apparatus are shown in figure 1(a).

A conical subsonic diffuser of 6° included divergence angle followed by a discharge duct having a controllable outlet plug was used throughout the investigation. Each of five perforated convergent diffusers was initially investigated without a cylindrical inlet, after which a shoulder was machined to receive three successively longer cylindrical inlets (fig. 2). The diffusers investigated had contraction ratios S_1/S_2 of 1.40, 1.49, 1.53, 1.55, and 1.59. The internal contours (the same as those of similar contraction ratio reported in reference 2) included a 3/4-inch

straight lip before convergence (reduced to 1/2 in. with machining of shoulder) and an unperforated throat 1 inch in length and 1.542 inches in diameter. Inlet diameters and lengths of the diffusers are given in figure 1(b). Perforations, formed by a No. 43 drill (0.089-in. diam.), were countersunk to form sharp-edged orifices.

The longitudinal distributions of perforated area for each diffuser, presented as the dimensionless summation of the perforated area A/S_2 from the throat to the stations S/S_2 of the diffuser, are shown in figure 3. The perforation distributions are designated alphabetically by suffixes to the contraction ratio (for example, 1.40-A). Distribution A included sufficient perforated area for shock stability near the throat; distribution B was approximately the distribution of reference 2 that achieved maximum total-pressure recovery; distribution C was a theoretical distribution at a ratio of total perforated area to throat area slightly greater than the minimum value from reference 2 for which each diffuser was known to have swallowed the normal shock. The diffuser of contraction ratio 1.59 was investigated only with distributions A and B.

The diameter of the cylindrical inlets varied with the diffuser to which they were attached. Lengths of 3, 5, and 7 inches were used, which made the total cylindrical lengths before convergence approximately 2, 3, and 4 inlet diameters, respectively. The 5-inch inlet was omitted for the part of the investigation involving perforation distribution C. For each configuration, the variation of pressure recovery with mass-flow recovery was obtained by controlling the back pressure in the discharge duct with the conical outlet plug.

Supplementary runs were made using cylindrical inlets of lengths $4\frac{3}{4}$, $7\frac{1}{2}$, $9\frac{1}{2}$, and $11\frac{1}{2}$ inches mounted directly to the subsonic diffuser. The position of the internal shock in each of these inlets was varied by back-pressure control with the outlet plug.

The apparatus was so oriented that the cylindrical inlets ahead of the perforated diffusers were alined to the tunnel axis within $\pm 0.05^\circ$ vertically and $\pm 0.2^\circ$ horizontally. Previous tunnel calibration indicated an average upward flow inclination of approximately 0.1° at the cylindrical inlets. Those cylindrical inlets mounted directly to the subsonic diffuser were alined with entering flow by equalization of four internal static pressures measured at 90° circumferential stations located 1/2 inch from the inlet lip.

Internal static pressures were measured at the throat of the supersonic diffusers and along the cylindrical inlets. The tubing for the inlets was externally oriented to cause minimum flow disturbance in the vicinity of the perforations. Pressures in the discharge duct were measured by means of a 40-tube pitot-static rake from which the total-pressure recovery P_3/P_1 and the mass-flow recovery m_3/m_1 were obtained. All pressures were photographically recorded from a differential-type manometer board using tetrabromoethane with an approximate specific gravity of 2.95.

ANALYSIS OF POWER REQUIREMENTS

In evaluating the over-all performance of perforated diffusers, it is necessary to consider the disposition of the air bled through the perforations. In aircraft installations, the adverse effect of the bleed on net thrust must be considered. For applications as wind-tunnel second throats (suggested in reference 1) attention must be given to the equipment and power necessary to pump the bled mass flow m_b up to atmospheric or some convenient discharge pressure; in addition there are the usual requirements for the pumping of the recovered mass flow m_3 which reaches the subsonic diffuser.

The data of this investigation may be used to evaluate the performance of perforated diffusers as second throats by assuming the air entering the cylindrical inlets affixed to the diffusers to have been isentropically accelerated through a supersonic nozzle. The operating requirements of these simulated wind tunnels may then be defined as the sum of (1) the power required to compress the recovered mass flow m_3 in the reciprocal ratio P_1/P_3 of the recovered total pressure; and (2) the summation for the entire supersonic diffuser of the power required to compress the increment of mass flow bled by each perforation up to the upstream reservoir pressure P_1. Instrumentation readily permits evaluation of the first mentioned power. Analysis of bleed power, however, is complicated by the impossibility of measuring either the local internal static pressure and bled mass flow at individual perforations or the loss in kinetic energy across the perforations. A conservative approximation to actual bleed power requirements may be made from the experimental data by considering a tunnel installation wherein the perforated second throat is enclosed by an annular reservoir maintained at a pressure sufficiently low to induce exit flow through all perforations. Then, if recovery of dynamic

pressure is neglected, the bleed power can be represented by compression of the entire bleed flow m_b from the test-section static pressure p_1 to the test-section total pressure P_1.

The power requirements for the models of this report are computed on the basis of isentropic enthalpy change with the assumption of adiabatic flow. Thus, the conservative approximation to bleed-power requirements yields the following expression for the complete configurations:

$$\text{Power} = m_3 c_p T_1 \left[\left(\frac{P_1}{P_3} \right)^{\frac{\gamma-1}{\gamma}} - 1 \right] + m_b c_p T_1 \left[\left(\frac{P_1}{p_1} \right)^{\frac{\gamma-1}{\gamma}} - 1 \right] \qquad (1)$$

A more detailed analysis of bleed power may be made if the variations of local internal static pressure and mass flow through the diffusers are theoretically determined. Then the single reservoir may be arbitrarily divided into smaller compartments, each maintained at a pressure sufficiently low to bleed all the contained perforations. The absolute value of these reduced pressures to be used in calculations would depend upon internal static pressures and that portion of the local dynamic pressure recovered across the perforations.

The evaluation of the configurations as wind-tunnel models is facilitated by the use of a power factor K defined by the expression

$$K = \frac{\text{Power}}{m_1 c_p T_1 \left[\left(\frac{P_A}{P_B} \right)^{\frac{\gamma-1}{\gamma}} - 1 \right]} \qquad (2)$$

where the numerator is computed from equation (1). The denominator represents the power required by a normal shock at the inlet mass flow m_1 and at theoretical total-pressure ratio P_A/P_B across the shock at the inlet Mach number. Thus, it represents the minimum theoretical starting power for a supersonic tunnel having isentropic subsonic diffusion. A reduction in power factor corresponds to a decrease in the theoretical tunnel operating power.

RESULTS AND DISCUSSION

In each of the cylindrical inlets, the gradual static pressure increase in the direction of flow was interrupted by peaks that indicated a series of weak internal shock reflections. It is presumed that the total-pressure losses through these internal disturbances had negligible effect on the experimental results presented herein. The irregularity of static-pressure distributions, however, precluded use of the isentropic channel flow relations for the calculation of approximate boundary-layer displacement thicknesses.

The total-pressure and mass-flow recovery characteristics of the diffusers investigated without cylindrical inlets with perforation distribution A showed close correlation with results for the similar distribution examined in reference 2. When initial boundary layer was introduced, only the diffuser of 1.59 contraction ratio showed marked deviation in performance in that it failed to swallow the normal shock. Increasing the perforated area to the 1.59-B distribution was necessary to permit the establishment of supersonic flow in this diffuser.

Addition of the cylindrical inlets to the diffusers affected the variation of total-pressure recovery P_3/P_1 with mass-flow recovery m_3/m_1 as shown in figure 4, which presents typical data (perforation distribution 1.49-B) for shock-swallowed conditions. In agreement with the results of references 1 and 2, the peak recovery was obtained in all cases with the shock located as far upstream of the throat as possible without entering the region of instability. As the shock was moved to the throat from this location, the total-pressure recovery decreased while the mass-flow recovery increased to a supercritical or constant value. The pressure recovery P_3/P_1 and its reciprocal P_1/P_3 that exist when supercritical flow is first established, that is, shock at throat entrance, are defined as the critical pressure recovery and the critical pressure ratio, respectively.

The measured values of peak total-pressure recovery and corresponding mass-flow recovery for each configuration are plotted as a function of cylindrical length-diameter ratio C/D in figure 5. The data points shown at approximately 0.4 diameter indicate results obtained from the initial runs without cylindrical inlets. The combination of friction losses in the cylinders and changes in separation and shock losses in the diffusers produced decreases of the order of 2.0 percent in peak P_3/P_1 for the five diffusers over the range of cylinders employed. This same order

of decrement is shown for each perforation distribution. The mass-flow recovery at peak pressure ratio also decreased with increasing cylindrical length-diameter ratio as shown in figure 5. This last reduction can be attributed in part to the greater efficiency of the perforations in bleeding the reduced energy air of the boundary layer. In addition, the position of the shock at peak recovery moved upstream with increasing entrant boundary layer. As a consequence, the increased subsonic bleed behind the shock further contributed to the reduction in mass-flow recovery.

Conservative power requirements of the simulated wind tunnels as computed by equation (1) indicate that, for a given configuration, minimum power is found at the critical pressure recovery with the shock positioned at the entrance of the diffuser throat. For this shock position the reduction in bleed flow and hence bleed power from that at peak pressure recovery offsets the adverse effect on power of the decrease in pressure recovery from the peak value. The flow parameters at minimum power in terms of the critical total-pressure ratio P_1/P_3 and the corresponding relative bleed flow m_b/m_1, are presented in figure 6 as functions of the cylindrical length-diameter ratio C/D. For a given perforation distribution, an increase in diffuser contraction ratio tended to decrease the operating pressure ratio but at the expense of a greater bleeding of mass flow through the perforations. Perforation distribution C, which gave the least range of shock stability in the convergent portion of the diffuser, is seen to require the highest operating pressure ratio but the least bleed flow. For all configurations this distribution required pressure ratios of less than 1.2 and bleeding of less than 8 percent of the mass flow m_1 of the simulated tunnel test section. Increasing the boundary layer to a maximum resulted in an average increase for the five diffusers of approximately 3 percent for critical P_1/P_3. The corresponding increase in relative bleed flow m_b/m_1 of about 50 percent represents an approximate decrease in supercritical m_3/m_1 of 2 percent.

The power factor K (equation (2)) was computed for minimum power conditions from the data of figure 6 and is presented in figure 7 as a function of the total configuration length-diameter ratio L/D. The marked increase in power factor with increasing boundary layer reflects the influence of the increase in critical pressure ratio and relative bleed flow noted in figure 6. For each diffuser the least operating power requirements were indicated for perforation distribution C, which was the distribution closely approximating the minimum perforated area necessary for swallowing the normal shock. Thus, in effecting over-all power reductions, the

previously noted low bleed-flow requirements of perforation distribution C more than compensate for the associated higher critical pressure ratios. The important influence on K of the bleed-power requirements is also evidenced by the lack of an appreciable superiority of any one diffuser despite an improvement in critical pressure ratios with increasing contraction ratio.

A more optimistic bleed power determination than that expressed in equation (2) might be expected to favor the more highly contracted diffusers with their lower critical pressure ratios. Accordingly, the bleed-power requirements of configurations 1.40-C, 1.49-C, and 1.55-C combined with the shortest cylindrical inlets were investigated using a theoretical determination of the internal diffusion process. Instead of the previously considered single bleed reservoir, four annular reservoirs of equal width were assumed and the total bleed power was taken to be the sum of the powers required for each. The results of this analysis are shown in figure 8, where power factors are presented as functions of diffuser contraction ratio. Three methods of computing bleed power are designated in the figure as follows: (A) single annular reservoir, no recovery of dynamic pressure across perforations (equation (2)); (B) four annular reservoirs, internal supersonic diffusion considered, no recovery of dynamic pressure across perforations; and (C) same as (B) except for recovery of one-half of the local dynamic pressure across the perforations. The dashed curve represents the power factor for the recovered mass flow m_3 considered alone.

Whereas no appreciable difference in total power is shown for diffusers 1.40-C and 1.55-C for method (A), a 15-percent reduction is produced by the greater contraction using method (C). Accompanying this decrease in total power with increasing contraction ratio is a reduction of 32 percent in the power required for the recovered mass flow. Figure 8 significantly shows that the exact choice of the contraction ratio for optimum power economy requires precise experimental determination of bleed-flow parameters.

The power factor K represents a comparison of the performance of the second-throat configurations to that of an ideal noncontracted tunnel. Thus, it allows quantitative interpretation of the power requirements of the models. Comparison with actual noncontracted tunnels of similar scale, however, reveal more clearly the power economies effected by use of the perforated second throat. In order to furnish data for this comparison, the supplementary runs involving straight cylinder-subsonic diffuser combinations were made. These data are shown in figure 9 as a variation of total-pressure recovery with shock position in each of the four cylinders examined.

For each configuration, the very marked decrease in total-pressure recovery as the shock was moved closer to the subsonic diffuser (away from the inlet lip) indicates an effect not readily predictable from a consideration of the shock Mach number alone. In order to more easily discern the influence of other factors on total-pressure recovery, the data of figure 9 were cross-plotted in figure 10, where the variation of P_3/P_1 is shown with cylindrical length-diameter ratio L/D at constant values of x/D and y/D which represent the distance of the shock ahead of the subsonic diffuser and behind the inlet lip, respectively.

A simple diverging inlet used on this subsonic diffuser for pressure-rake calibration purposes gave a total-pressure recovery of 0.750 with the shock just inside the lip (theoretical normal shock recovery at $M = 1.9$ is 0.767). Thus, the curve of $x/D = 0$ (shock at the subsonic diffuser entrance) has presumably decreased from 0.750 at $L/D = 0$ to 0.510 ($L/D = 3$) by the addition of 3 diameters of straight section ahead of the shock. The addition of increasing lengths of straight section x/D behind the shock (keeping $y/D = 3.0$), however, increases the pressure recovery to a value of 0.714 at $x/D = 2.5$. Inasmuch as friction losses cannot account for the magnitude of the initial decrease nor for the return to the higher recovery, it is apparent that (1) the interaction of the shock and the boundary layer at the subsonic diffuser entrance produces flow separation of serious consequence to pressure recovery, and further that (2) the subsequent addition of straight sections behind the shock produces increasing improvement in diffuser entry conditions by allowing prior reattachment of separated flow. Apparently adding sufficient straight-section length between the shock and subsonic diffuser gives pressure recoveries that closely approach normal shock values (considering the presence of friction losses).

The upward trend in the curve of $x/D = 0$ with increasing L/D may be attributed to the slight reduction in shock Mach number accompanying its downstream movement. The improvement in pressure recovery across the shock appears to overshadow the increasing friction losses that are presumably responsible for the downward trend of the curves of higher x/D values.

Comparisons of the relative efficiencies of the simulated contracted and noncontracted tunnels can be indicated as a ratio of their respective operating power requirements (hence a ratio of power factors). The operating pressure ratios P_1/P_3 and thus power requirements of the noncontracted configurations, however, are dependent on shock position in the constant-area section.

Comparisons of the two types of tunnel were accordingly made at the same simulated test-section length in diameters and for shock positions x/D corresponding to the length l/D (fig. 1(b)) of the perforated diffusers. The ratio η of contracted to noncontracted power requirements thus computed is shown in figure 11. This figure gives further indication that the conservative method of evaluating power does not clearly establish optimum degree of contraction for the diffusers tested. For maximum entrant boundary layer to the diffusers, the greatest power savings (achieved with perforation distribution C) are approximately 25 percent of the noncontracted values. Greater reductions are again presumed possible dependent upon the exactness of bleed-power determination.

SUMMARY OF RESULTS

An investigation was conducted of mass-flow and total-pressure recovery characteristics of convergent-divergent supersonic diffusers with entrant boundary layer. Combinations of cylindrical inlets and perforated diffusers with a 6° conical subsonic diffuser were examined at a Mach number of 1.9.

Affixing 4 diameters of cylindrical section ahead of the diffusers affected the performance of the five diffusers to the extent of an approximate decrease of 2 percent in peak total-pressure recovery and supercritical mass-flow recovery. Variation of perforated-area distribution had little effect on the order of this decrease.

Simulated wind tunnels consisting of combinations of cylindrical inlets, perforated diffusers, and a subsonic diffuser indicated appreciable operating economy as compared with similar models investigated without geometric flow contraction. The indicated saving in total operating-power requirements depended on the methods used to evaluate the power necessary to bleed mass flow through the diffuser perforations. Using a conservative approximation of the bleed power, the diffuser configurations indicated operating-power requirements of 75 percent of those necessary for the noncontracted models. This saving was effected with operating total-pressure ratios of less than 1.2 and by removal through the perforations of less than 8 percent of the test-section mass flow.

Lewis Flight Propulsion Laboratory,
National Advisory Committee for Aeronautics,
Cleveland, Ohio.

REFERENCES

1. Evvard, John C., and Blakey, John W.: The Use of Perforated Inlets for Efficient Supersonic Diffusion. NACA RM E7C26, 1947.

2. Hunczak, Henry R., and Kremzier, Emil J.: Characteristics of Perforated Diffusers at Free-Stream Mach Number 1.90. NACA RM E50B02, 1950.

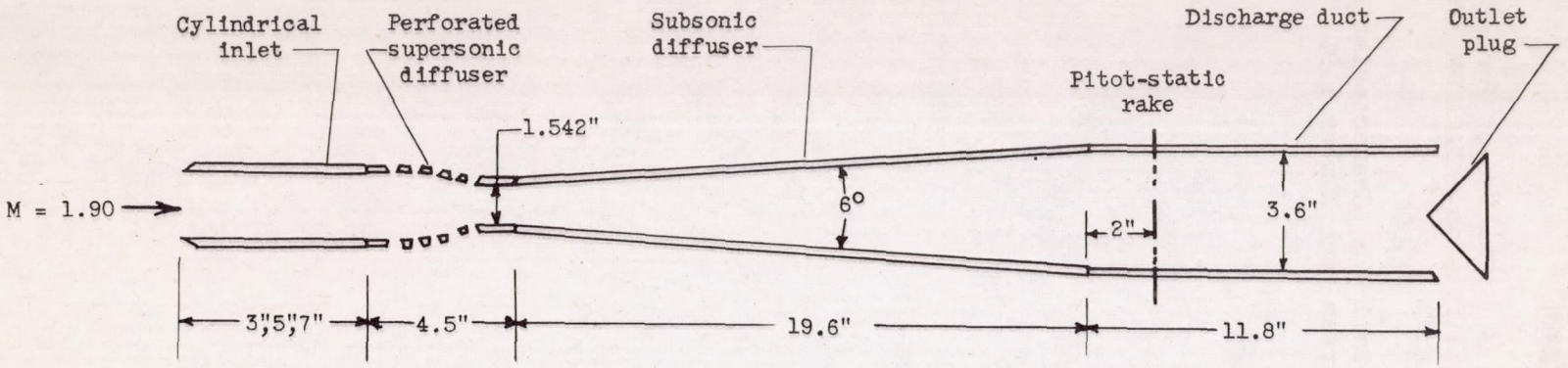

(a) Schematic assembly with perforated diffuser and cylindrical inlet.

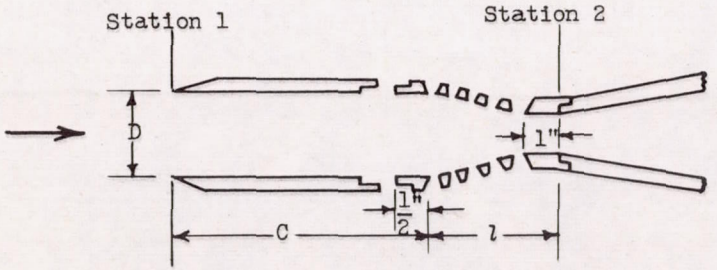

S_1/S_2	1.40	1.49	1.53	1.55	1.59
l/D	2.19	2.12	2.10	2.08	2.06
D	1.826	1.882	1.908	1.921	1.944

(b) Diffuser dimensions.

Figure 1. - Schematic diagram and dimensions of apparatus.

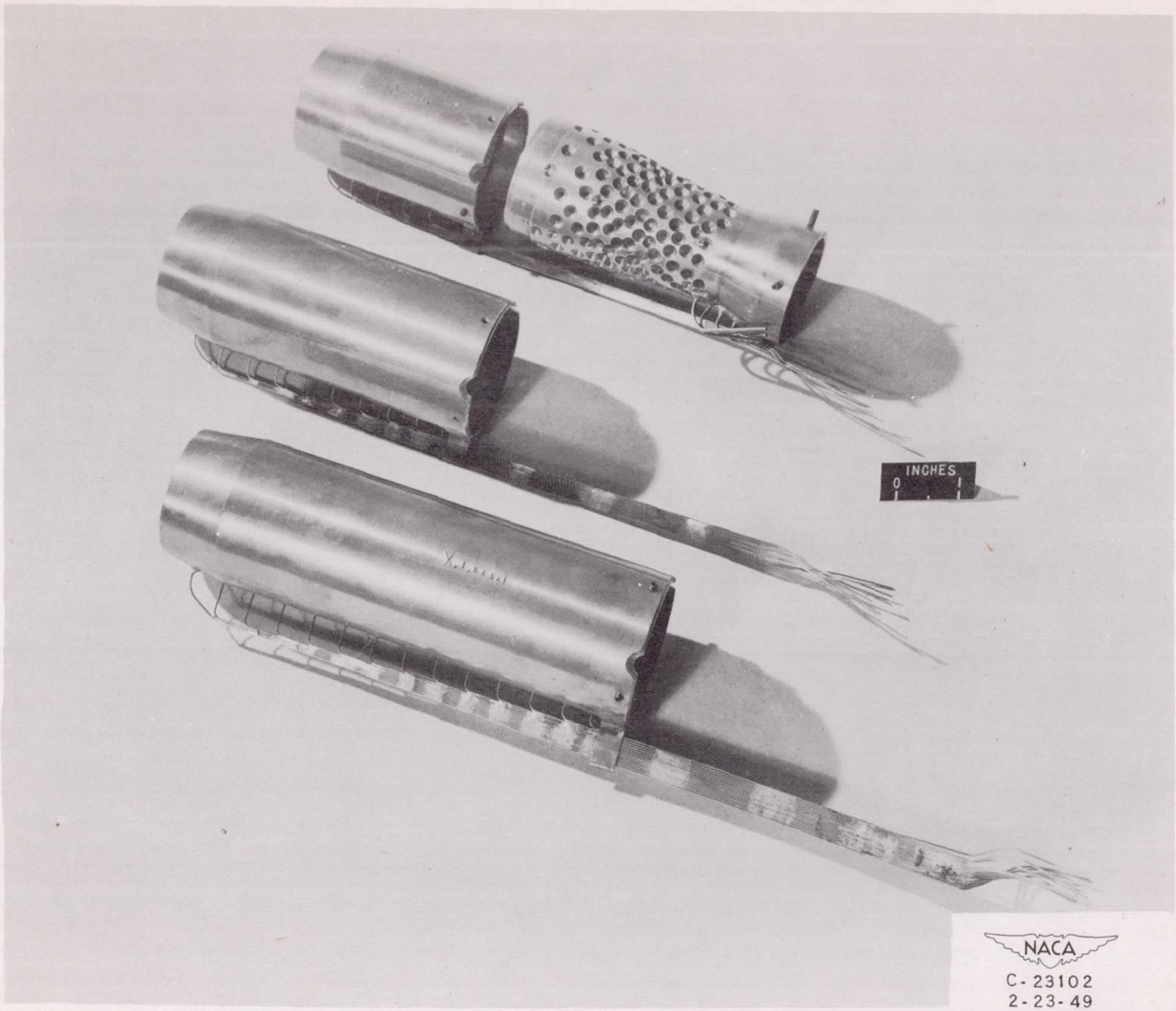

Figure 2. - Perforated supersonic diffuser with cylindrical inlets.

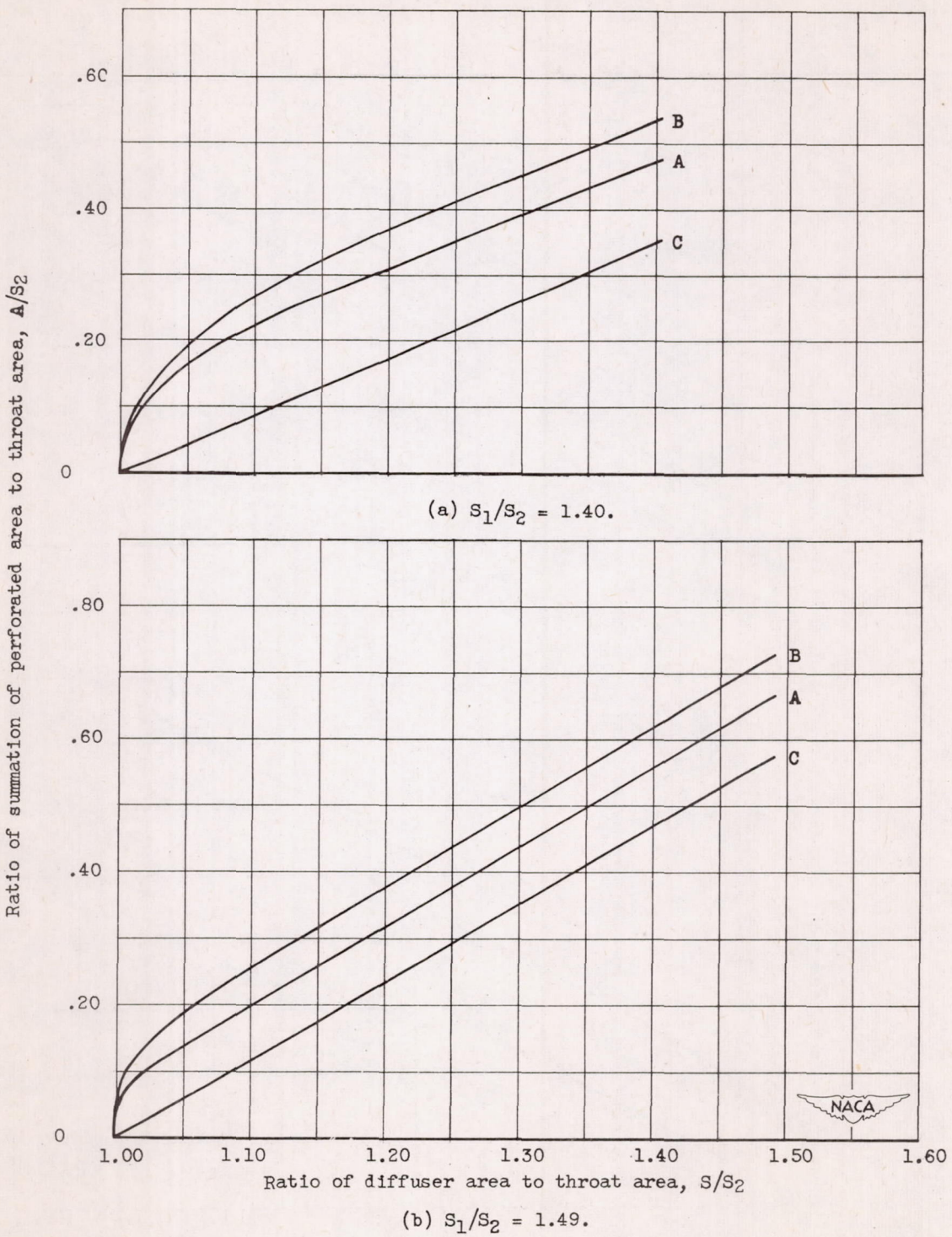

Figure 3. - Distribution of perforated area.

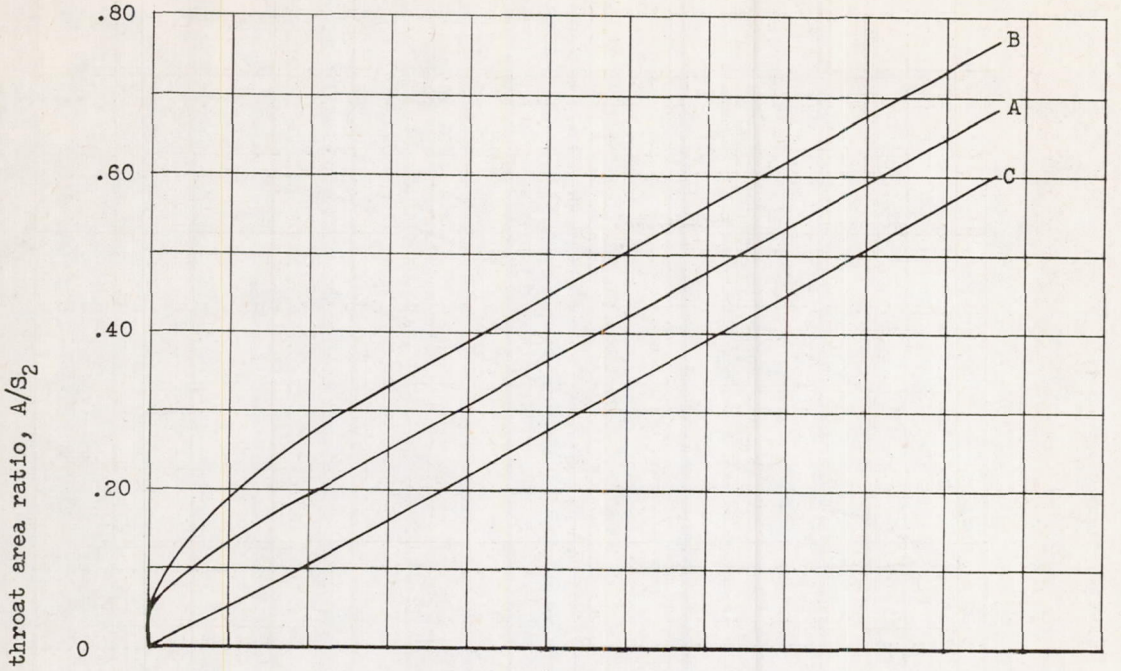

(c) S_1/S_2 = 1.53.

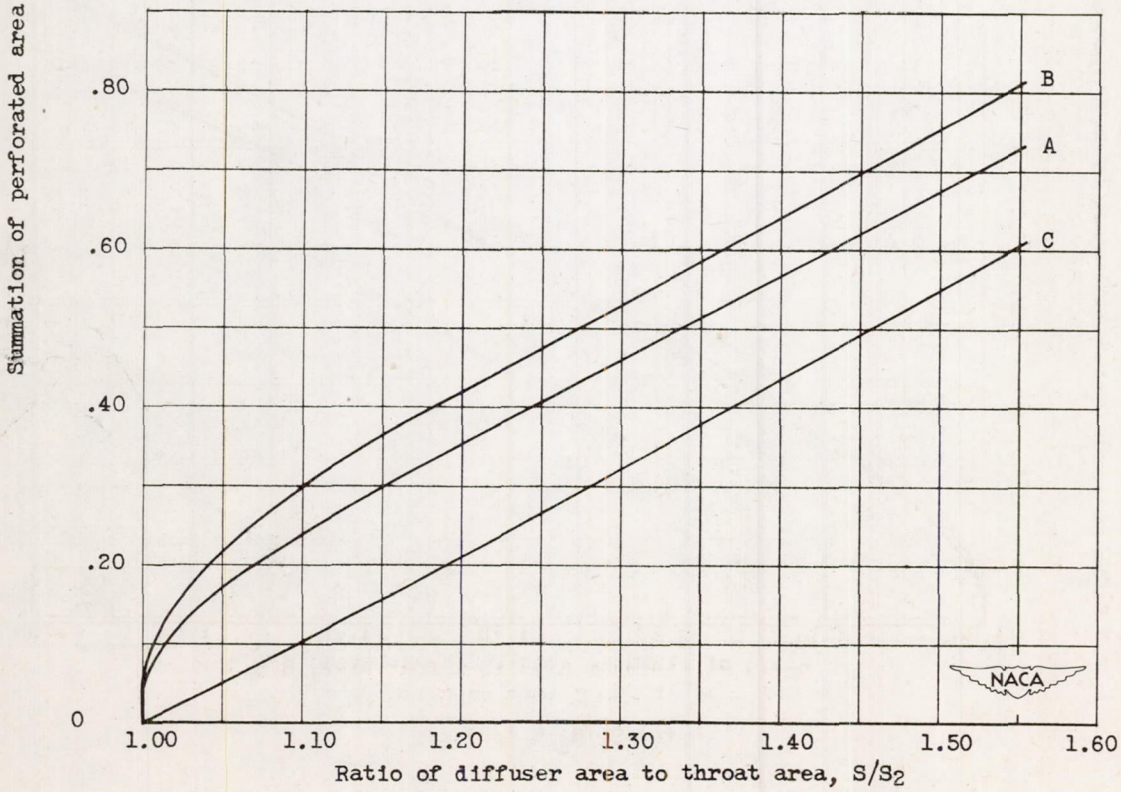

(d) S_1/S_2 = 1.55.

Figure 3. - Continued. Distribution of perforated area.

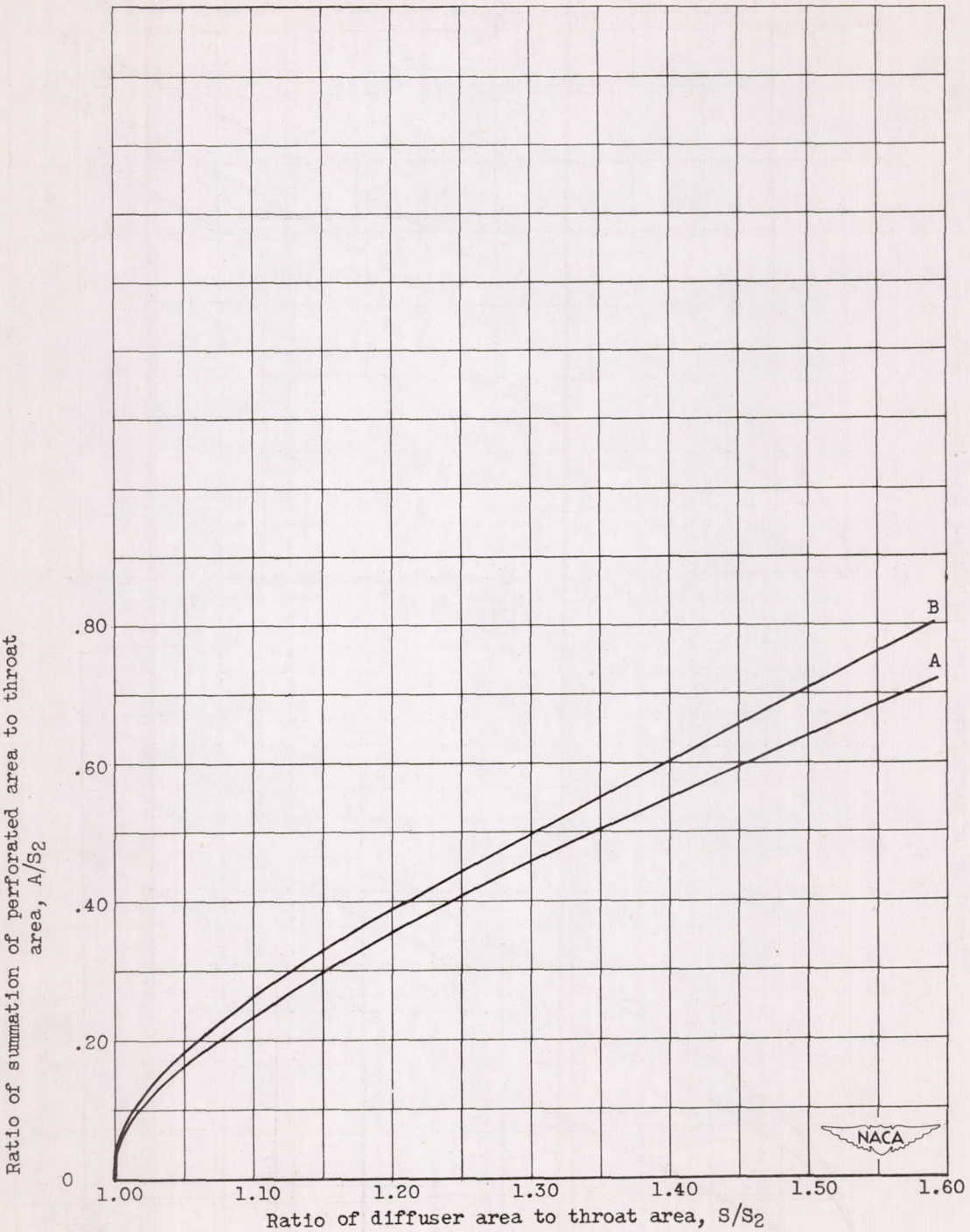

(e) $S_1/S_2 = 1.59$.

Figure 3. - Concluded. Distribution of perforation area.

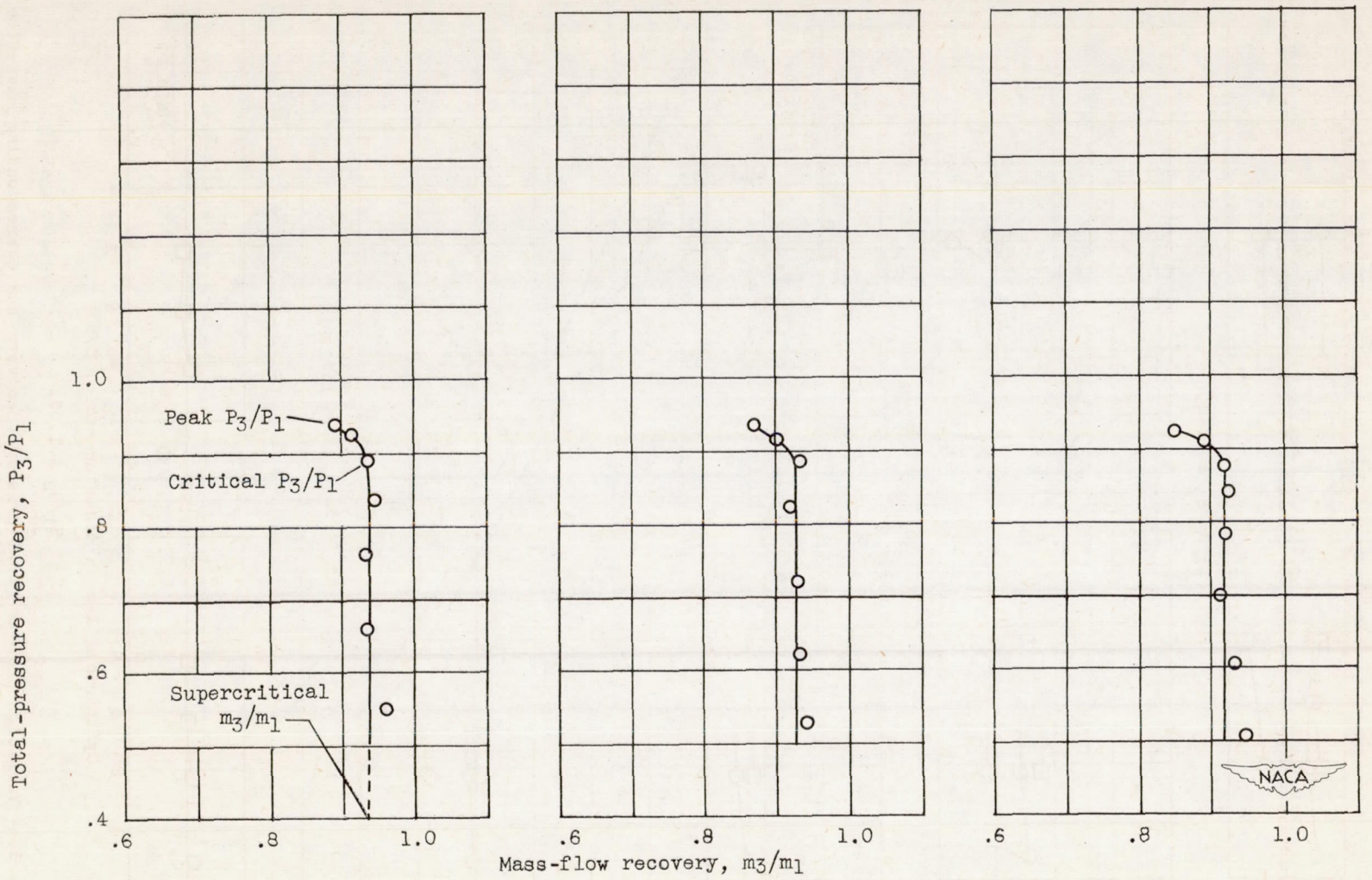

(a) C/D = 1.86. (b) C/D = 2.92. (c) C/D = 3.99.

Figure 4. - Variation of total-pressure recovery with mass-flow recovery for perforation distribution 1.49-B.

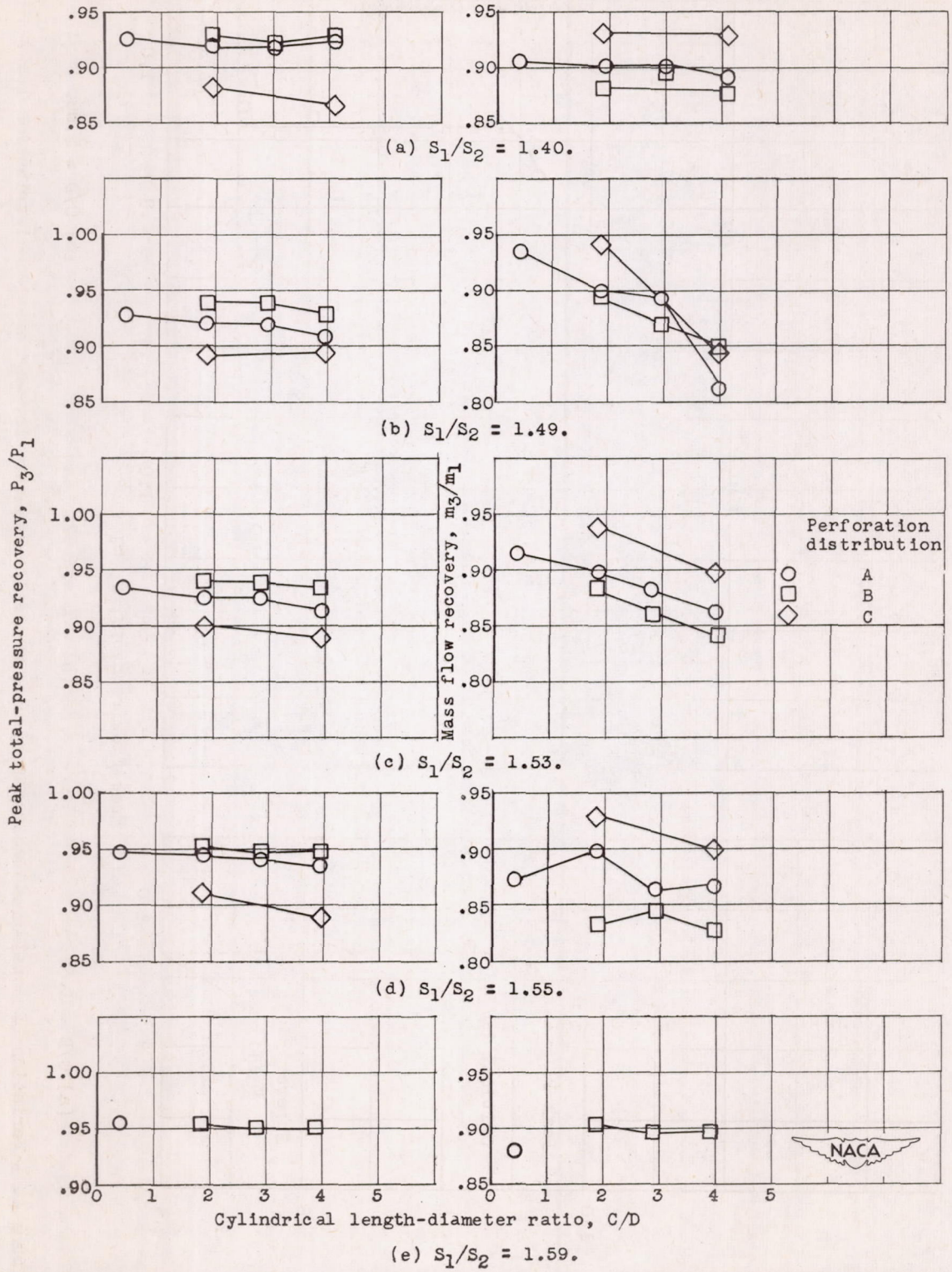

Figure 5. - Variation of peak total-pressure recovery and corresponding mass-flow recovery with cylindrical length-diameter ratio.

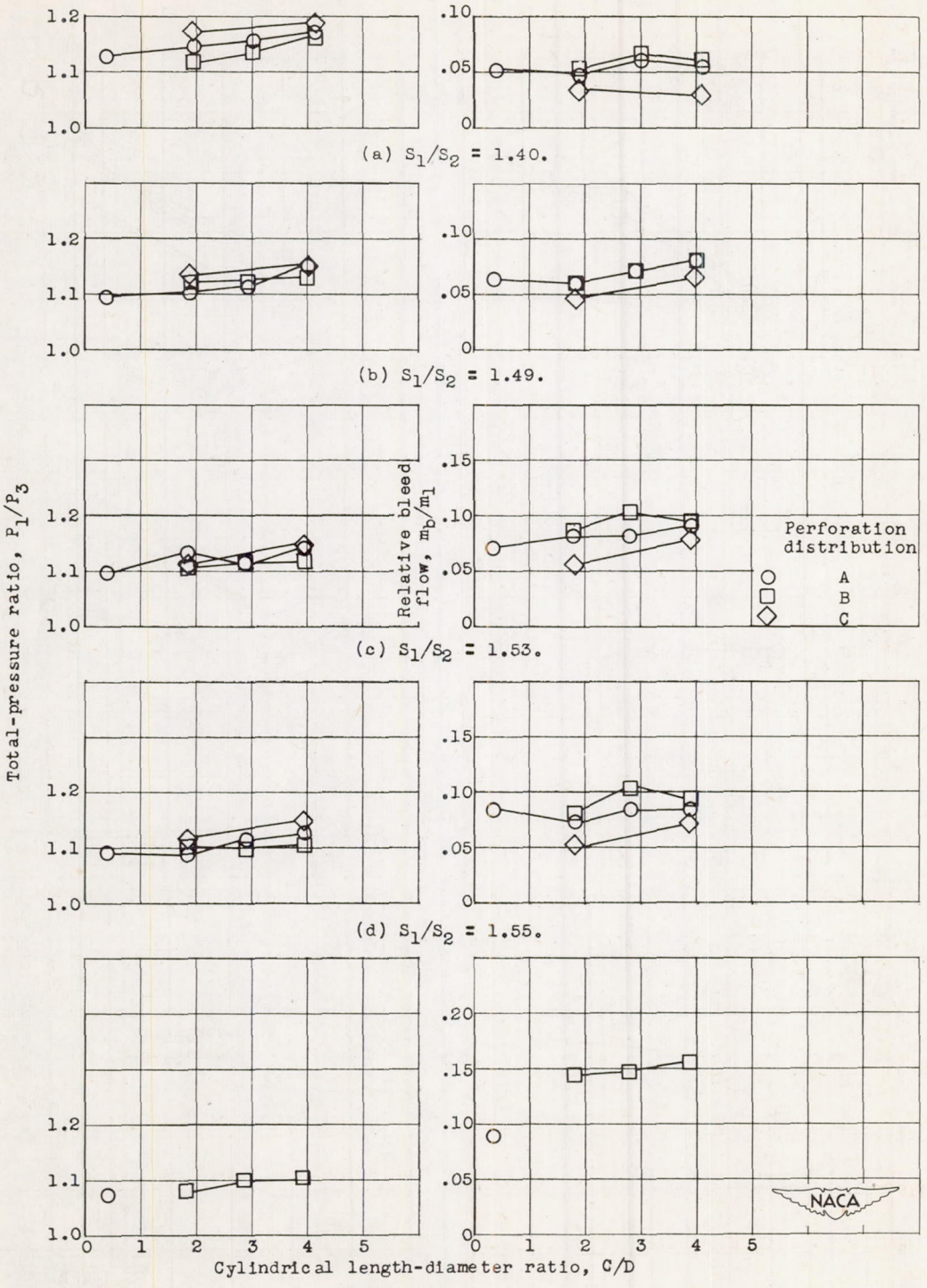

Figure 6. - Variation of critical total-pressure ratio and corresponding relative bleed flow with cylindrical length-diameter ratio.

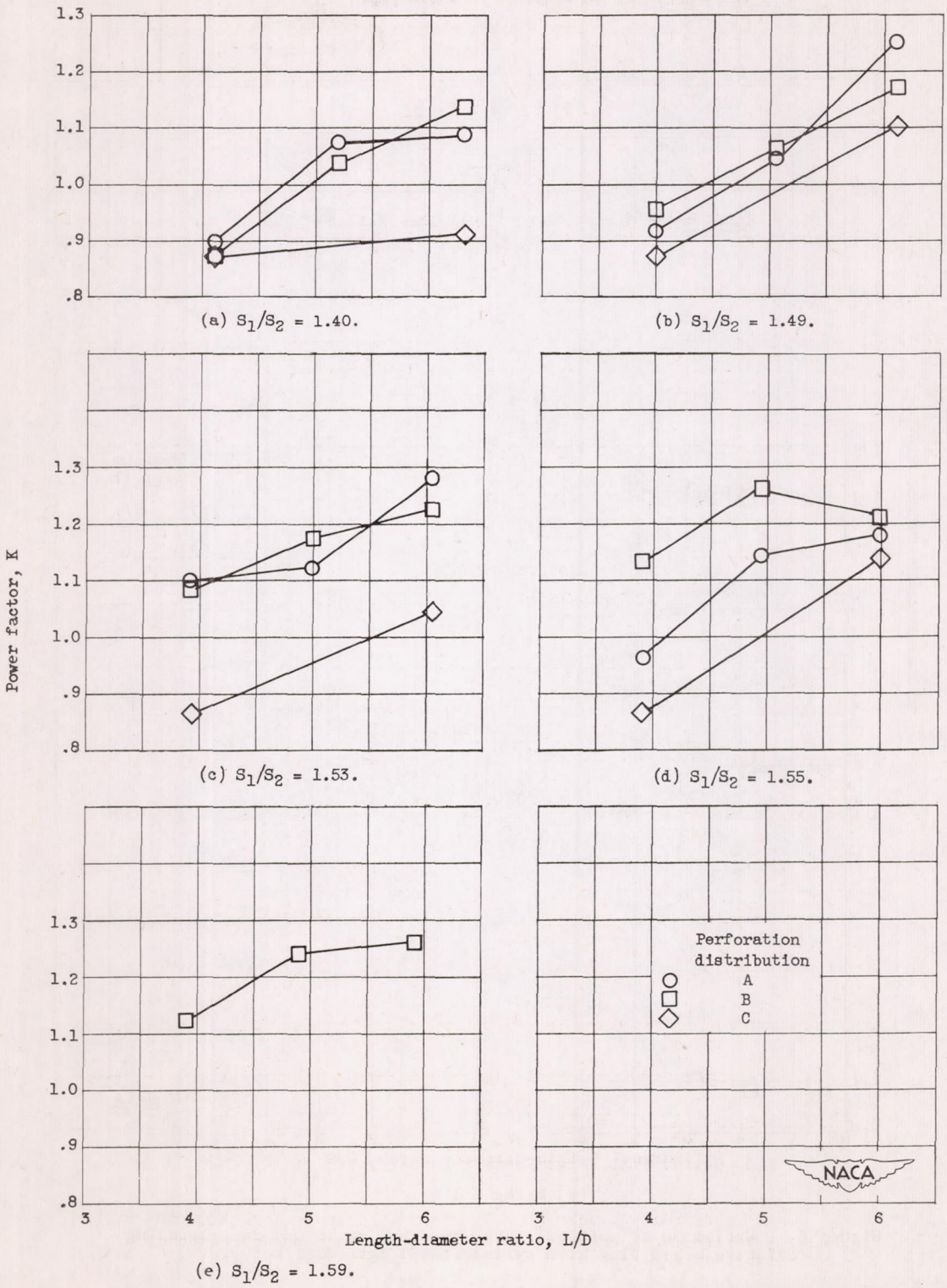

(a) S_1/S_2 = 1.40.

(b) S_1/S_2 = 1.49.

(c) S_1/S_2 = 1.53.

(d) S_1/S_2 = 1.55.

(e) S_1/S_2 = 1.59.

Figure 7. - Variation of power factor with total configuration length-diameter ratio.

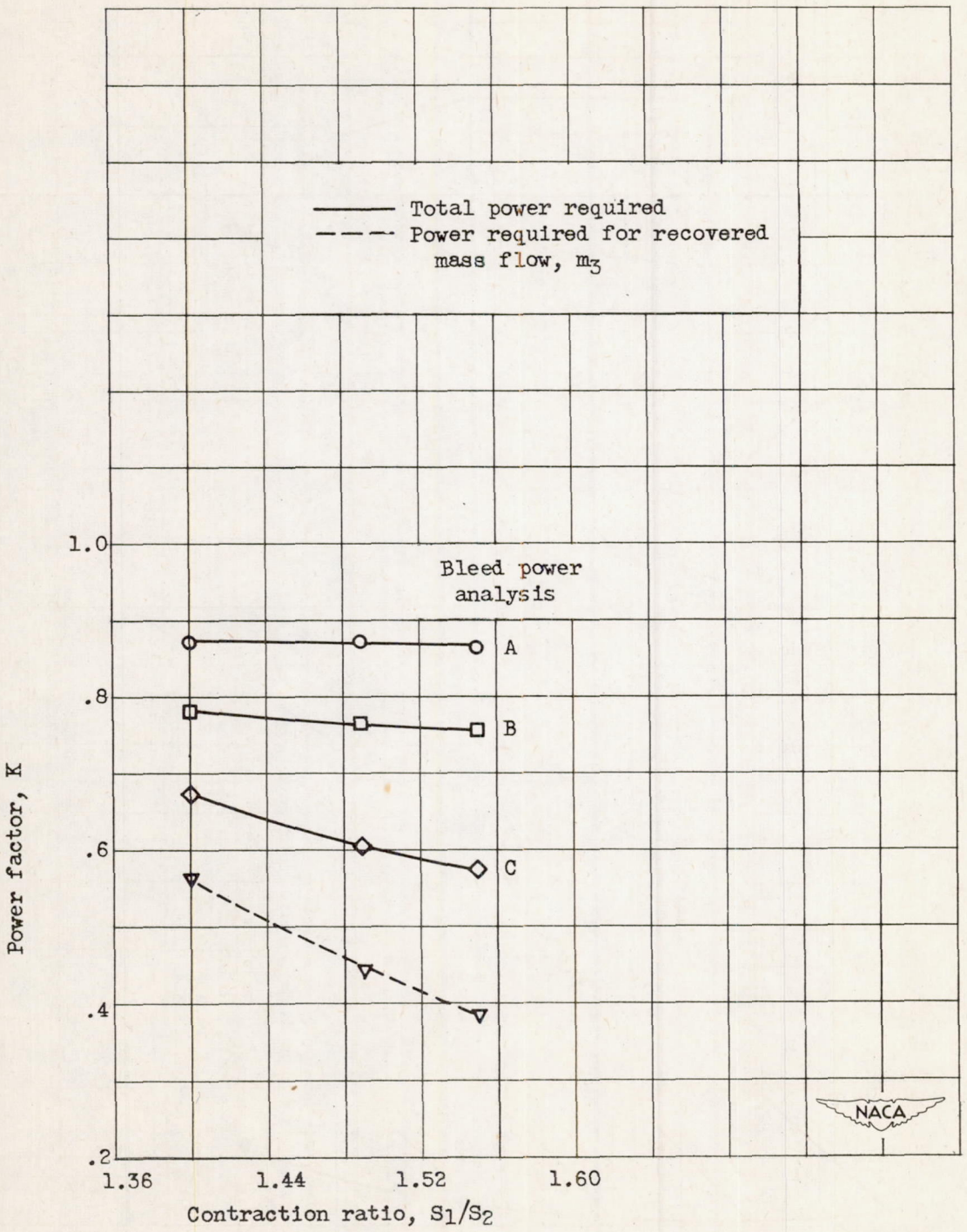

Figure 8. - Variation of power factor with diffuser contraction ratio for various methods of bleed power analysis.

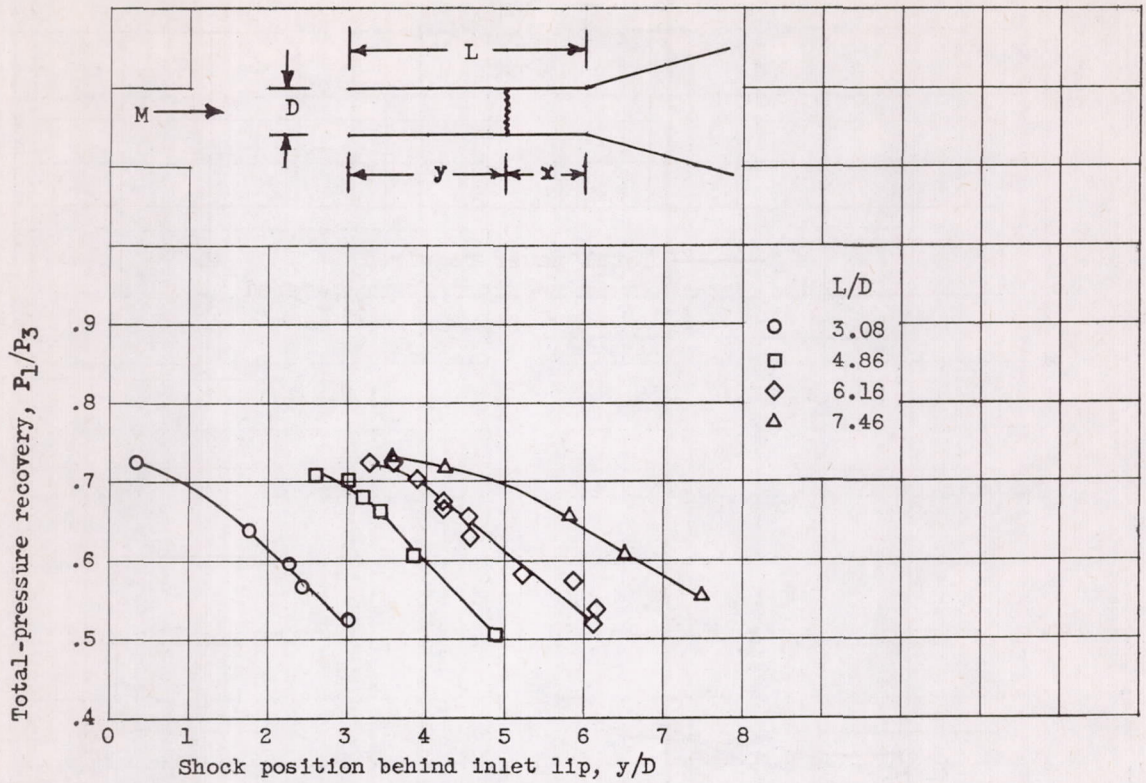

Figure 9. - Effect of shock position on total-pressure recovery.

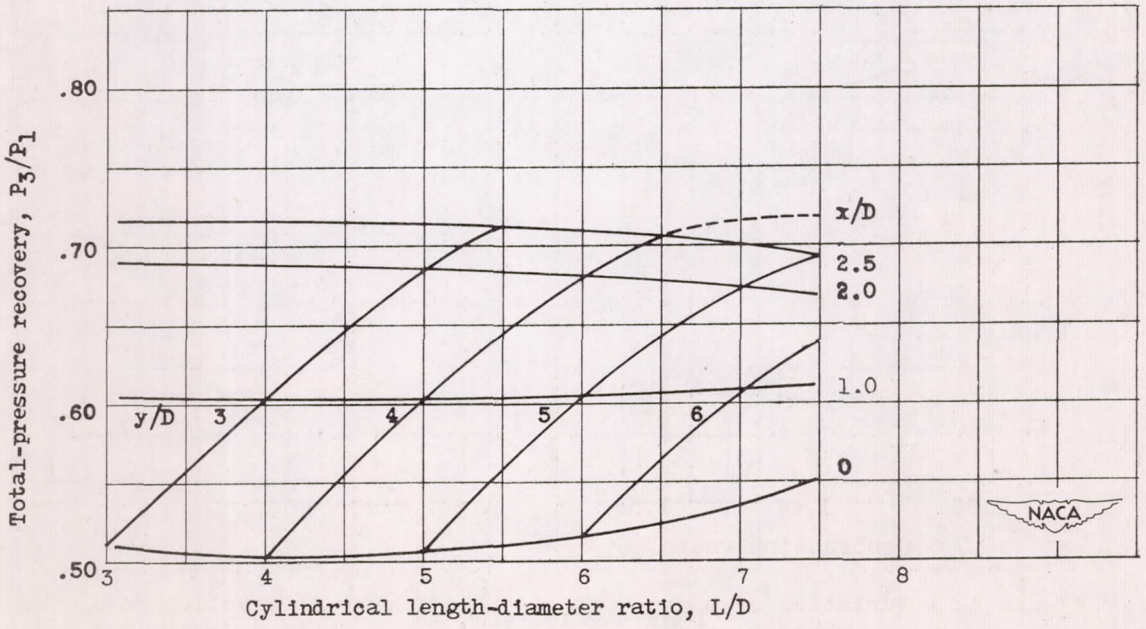

Figure 10. - Variation of total-pressure recovery with cylindrical length-diameter ratio.

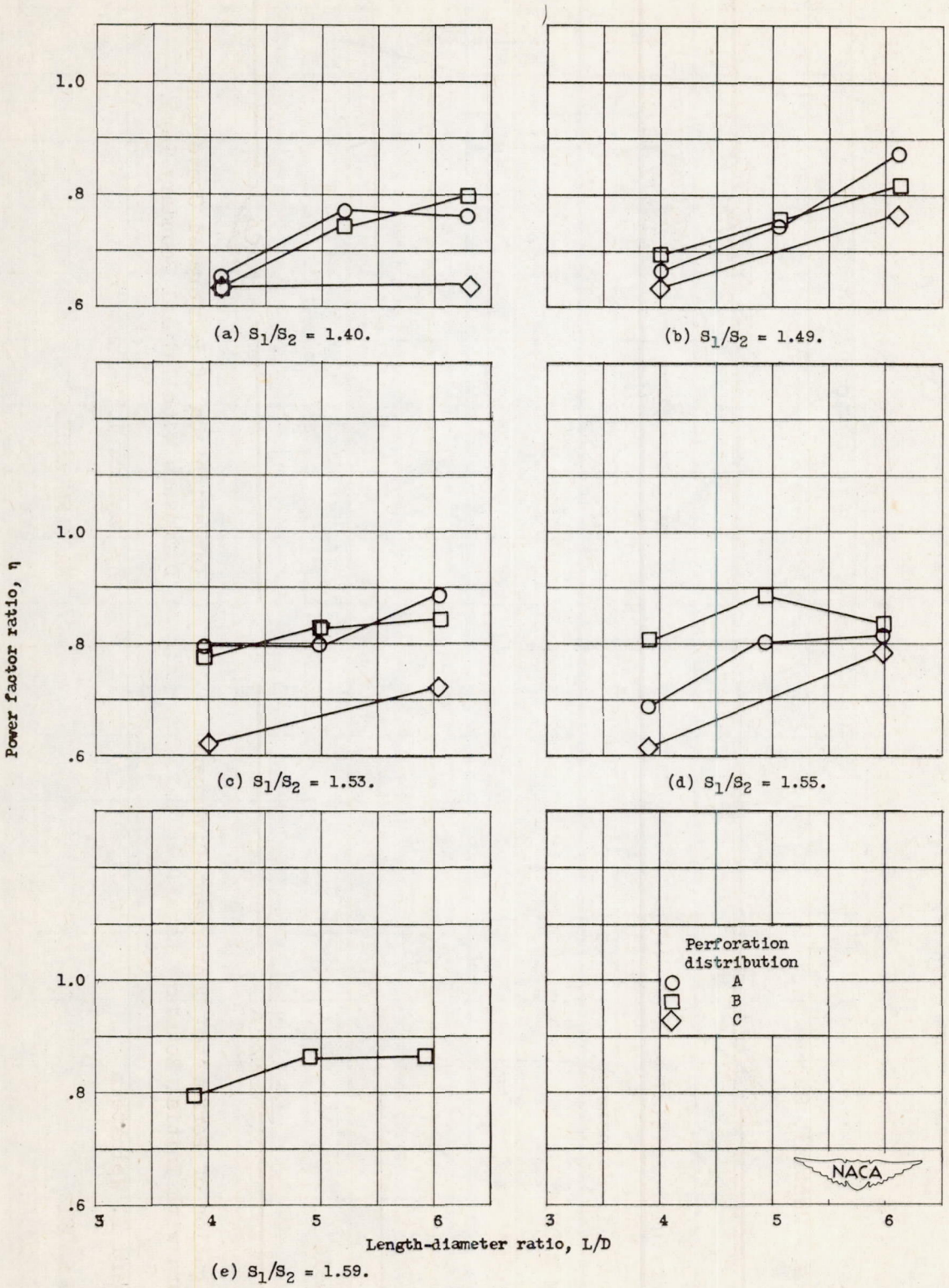

Figure 11. - Variation of power factor ratio with length-diameter ratio.